# Precision Orbit Determination for Errored Dynamic Models

Deepak Gaur
*Amity Institute of Space Science and Technology*
*Amity University*
Noida, India
deepakgauraerospace@gmail.com

Mani Shankar Prasad
*Amity Institute of Space Science and Technology*
*Amity University*
Noida, India
msprasad@amity.edu

***Abstract*— Precision orbit determination (POD) these days emerging to be one of the paramount research domains in spaceflight tasks, predominantly in altimetric tasks such as earth observing system mission: Ice, Cloud, and land Elevation Satellite (ICESAT) mission, satellite oceanography mission: JASON-1, and ICESat, and ocean surface topography mission: TOPEX/POSEIDON, which demands high precision (in centimeters) for radial orbits. Although, there exists limitations on orbit determination accuracy which are mainly because of the pre-existing unmodeled accelerations. To counter this problem and thus, boosting orbit determination precision values for error driven dynamic models, new methodologies have been surfaced. Two predominantly used algorithms to handle such tasks are State Noise Compensation (SNC) and Dynamic Model Compensation (DMC). Research presented aims at investigating and comparing the two algorithms to demonstrate the efficacy of both. To demonstrate benefits associated, an extension is incorporated in which DMC of 2nd-order is defined based on the assumption that characterization of unmodeled acceleration is possible in terms of differential equation of 2nd-order, followed by an example. As a result, it is observed that DMC of 2nd-order tend to deliver more precise estimate of position, velocity, as well as acceleration, along with better stability in comparison to conventional SNC and DMC. Moreover, a numerical simulation is conducted using DMC of 2nd-order with substandard tracking information of Lower Earth Orbit (LEO) satellite and on comparison of results with those incorporating Kalman filter exclusively, it is assessed that for substandard tracking, DMC of 2nd-order can perform efficiently delivering relatively precise trajectory estimation.**

***Keywords—Kalman Filter, Precision Orbit Determination, State Noise Compensation, Dynamic Model Compensation.***

## I. INTRODUCTION

Centuries before, interpretation of Kepler Laws of Planetary Motion gave birth to orbit determination. Although, shortage of near-earth objects precise monitoring information or data along with limitations on numerical computation, restricted orbit determination to theoretical development only, rather than real-time application to near-earth objects. Advent of high-performance computers, algorithms for accurate measurements and force models in past few decades led to substantial advancements in POD methods. Advances in scientific domains such as topography and oceanography has inspired POD to be significant research domain for spaceflight tasks, predominantly in altimetric missions which demands high precision (in centimeters) for radial orbits. For example, satellite oceanography mission: Jason-1, one of the altimetric mission, has a mission constraint of 1 centimeter for radial error. For accomplishment of such budget requirement, determination of POD computation, precise force models and productive result strategy is essential.

For POD quantification, tracking or monitoring data gathered by onboard GPS receiver are used. Although, due to error range limitation to few centimeters, data computed via Satellite laser ranging (SLR) which tends to be highly accurate, still not considered as a good choice due to highly sparse nature (i.e. for Geosynchronous Earth Orbit (GEO) satellite it is significant hours/pass). Furthermore, another satellite navigation system, Doppler Orbitography and Radio-positioning Integrated by Satellite (DORIS) system along with altimetric sweep, employed for POD computation by few satellites, resulted in highly precise data, but white noise and color noise affected the data. At the same time, in few past decades, extensive development has been recorded for force models. Although, models for tide, gravity, radiation pressure, and atmospheric drag are normally used for POD computation, they are still far from accurate to delineate the accurate physical procedure. Particularly, in situations like swift geomagnetic storms, and interplanetary shocks, where high-altitude winds, and atmospheric density changes very rapidly, making it impossible to accurately model them. So, although accurate monitoring data already exists, there still lies necessity for development of productive result strategy to handle such existing errors present in dynamic models.

TABLE I. DIFFERENT SATELLITES POD RESULT COMPARISON

| SATELLITE | RADIAL RMS |
|---|---|
| JASON-1 | <1 cm |
| ICESAT | ~ 2 cm |
| TOPEX/POSEIDON | 3 ~ 4 cm |
| CHAMP | ~ 17 cm |

Numerous satellites like Jason-1, ICESat, TOPEX/Poseidon, and CHAMP have accomplished this milestone of POD restricted orbit range error to few centimeters [1 - 6]. Different satellites POD results have been summarized in Table I. Prime objective of this research is POD methodology development, primarily in presence of unmodeled accelerations.

## II. SOLUTION METHODOLOGY

### A. Solution Methodology Development

For handling dynamic models which are imperfect in nature, various methods have been brought to existence, out of which, SNC and DMC are considered to be the most important methods [7].

978-1-7281-2068-3/19/$31.00 ©2019 IEEE

SNC functioning depends on assumption that white noise is the error existing in dynamic model, which implies, stochastic dynamics affects the state parameters. SNC yields a source of estimation enhancement via unknown random acceleration compensation.

In comparison to SNC, DMC is comparatively sophisticated. It relies on the assumption that it is possible to characterize the unknown acceleration as a linear stochastic differential equation of 1st-order, which comprises of deterministic acceleration component and a purely random term. However, it is possible to regenerate acceleration and carry out improved state vector estimation.

*B. Methods Evaluation*

Process noise included linearized system general equation is

$$\frac{dx}{dt} = A(t).x(t) + B(t).u(t) \tag{1}$$

Process noise matrix is represented by the term $u(t)$, and

$$\mathrm{E}\left[u(t)\right] = 0 \tag{2}$$

$$\mathrm{E}\left[u(\tau).u^{T}(\tau)\right] = Q(t).\delta(t-\tau) \tag{3}$$

Covariance matrix for the process noise is represented by the term $Q(t)$, and represented as

$$Q = \begin{bmatrix} \sigma^2_{d^2x/dt^2} & 0 & 0 \\ 0 & \sigma^2_{d^2y/dt^2} & 0 \\ 0 & 0 & \sigma^2_{d^2z/dt^2} \end{bmatrix} \tag{4}$$

Here $\sigma^2_{d^2x/dt^2}$, $\sigma^2_{d^2y/dt^2}$, $\sigma^2_{d^2z/dt^2}$ are taken as constants and preliminary estimation of these, in general, relies on the limited information of dynamic process and can be made better via trial & error method.

Solving (4), state estimate propagation is the same as excluding process noise, which is

$$\overline{x}(t_k) = \phi(t_k, t_{k-1}).\hat{x}_{k-1} \tag{5}$$

But the process noise will influence the variance-covariance matrix

$$\overline{P}(t_k) = \phi(t_k, t_{k-1}).P_{k-1}.\phi^{T}(t_k, t_{k-1}) + \int_{t_{k-1}}^{t_k} \phi(t,\tau).B(\tau).Q(\tau).B^{T}(\tau).\phi^{T}(t,\tau).d\tau \tag{6}$$

Hence, Kalman filter derived results will vary from one excluding process noise. For SNC, consideration is limited to exclusive presence of random noises on acceleration, which means, both state vector and matrix 'A' will still be equivalent as excluding process noise. DMC relies on assumption that characterization of unknown acceleration is possible in terms of linear stochastic differential equation of the 1st-order

$$\eta(t) = \eta_0.e^{-\beta(t-t_0)} + \int_{t_0}^{t} e^{-\beta(t-\tau)}u(\tau).d\tau \tag{7}$$

The deterministic part $\eta_D(t) = \eta_0.e^{-\beta.(t-t_0)}$ can be summed up to the state vector and approximated along with the position and the velocity. Thus, resulting state vector turns to be

$$X(t) = \begin{bmatrix} X \\ \dot{X} \\ \eta_D \end{bmatrix} \tag{8}$$

Further, the dynamic equation can be represented same as (1). However, the effects of $\eta$ have been inducted in modified $A$ matrix. For comparing SNC's and DNC's stability and effectiveness, an example is taken into consideration to demonstrate underlying difference within the two algorithms [8]. Considering an object moving at a constant velocity of 10 m/sec along the positive x-axis direction. Sinusoidal acceleration at t = 0 is given by the term $\eta(t) = \frac{2\pi}{10}\cos\left(\frac{2\pi}{10}t\right)$ meter/second, in x-axis direction, is summed up to the object. A sensor, which relies on range rate and range measurements of standard deviation and zero mean of 0.1 meter/second and 1 meter respectively, is situated at $x = 10$ meters. Problem being linear in nature, thus, in place of EKF, Kalman filter is used to approximate the position and the velocity of the object, as shown in Fig.1, supposing perturbing acceleration is not known.

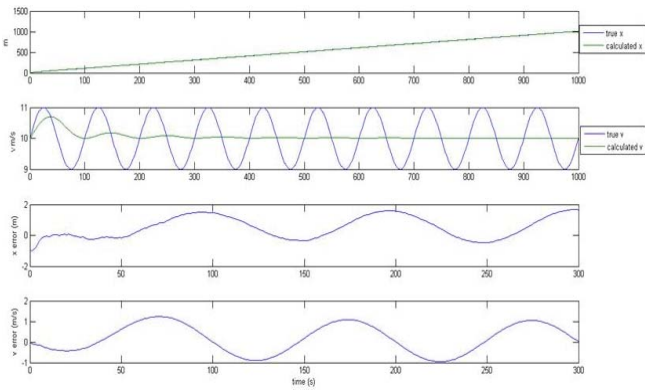


Fig.1. Comparison between Kalman filter applied calculated position and velocity w.r.t true position and velocity, along with Kalman filter applied position estimation error and velocity estimation error

As deduced from Fig.1, whereas sinusoidal acceleration being unmodeled, algorithm lacks compensation for acceleration which is unmodeled, eventually leading to failed estimation of the position and the velocity of the object along with substantial errors in position and velocity.

For compensating the unmodeled acceleration, the SNC in association with Kalman filter is carried out to deduce best approximation of the position and the velocity of the object

[9 - 10]. For approximate results optimization, the value of $\sigma$ needs to be adjusted. For present case, 0.4 is the optimal value for $\sigma$, $7.57*10^{-2}$ meter/second is velocity error RMS, and $9.83*10^{-2}$ meter is corresponding position error RMS [11 - 14].

From Fig.2 it can be seen that, multiple errors in approximation, as a result of imperfect dynamic model, have been corrected by SNC. Although, recovery of unmodeled acceleration cannot be carried out by SNC. Hence, DMC algorithm in association with Kalman filter is performed and approximation results are compared to those of SNC algorithm. Equations in such problem are

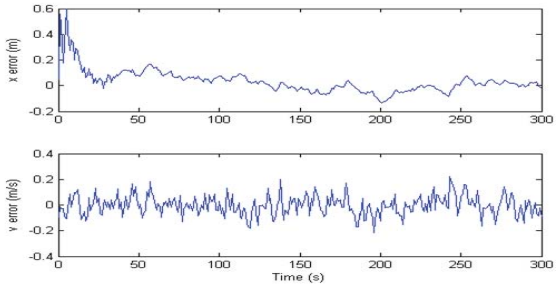


Fig.2. SNC + Kalman filter-based error estimation for position and velocity

$$\dot{x}(t) = A(t).x(t) + B(t).u(t); X(t) = \begin{bmatrix} X \\ V \\ \eta_D \end{bmatrix};$$

$$A = \begin{bmatrix} 0 & 1 & 0 \\ 0 & 0 & 1 \\ 0 & 0 & -\beta \end{bmatrix}; B = \begin{bmatrix} 0 \\ 0 \\ 1 \end{bmatrix};$$

$$E\left[u(t)\right] = 0; E\left[u(\tau).u^T(\tau)\right] = \sigma^2\delta(t-\tau) \quad (9)$$

In Fig.3, the results are demonstrated. Besides, for best approximation, optimization of both $\sigma$ and $\beta$ is carried which resulted in optimized value for $\sigma$ and $\beta$ to be 1.04 and 0.9 respectively [15 - 16]. Although position error RMS value is approximately equivalent with SNC, velocity error RMS value comparatively much smaller than SNC, thus, it can be deduced that even though SNC as well as DMC can produce finer position estimation, DMC tend to deliver more accurate estimation of velocity in vicinity of errored dynamic model.

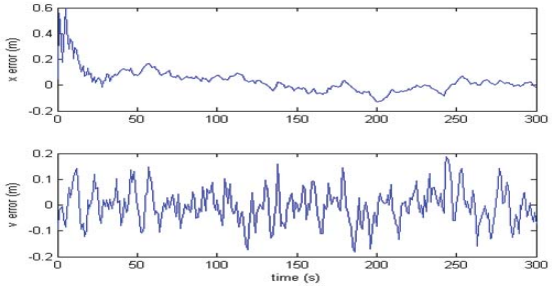


Fig.3. DMC + Kalman filter-based error estimation for position and velocity

Besides, an approximation of unmodeled acceleration can be yielded by DMC, which SNC fails to derive, as demonstrated in Fig.4. The value of acceleration error RMS comes out to be $2.424*10^{-1}$ meter/second$^2$. Hence, DMC offers potential of recovering unmodeled acceleration, which SNC lacks, thus in return improving the dynamic models.

On the contrary, choosing $\sigma$ value is a crucial application problem. Considering an example, where, since the true data are already present, to obtain best approximation, $\sigma$ is adjusted. Although, in real scenario, there is absence of sufficient knowledge about $\sigma$ and the true data which are important for commanding tuning process. Hence, for such compensation algorithm, sensitivity of $\sigma$ is a very crucial factor. For both SNC and DMC, computed values for position error RMS along with velocity error RMS for $\log(\sigma) = [-6:1:7]$, are presented in Fig.5.

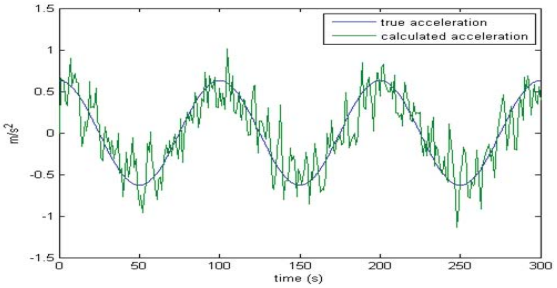


Fig.4. DMC + Kalman filter based unmodeled Vs calculated acceleration

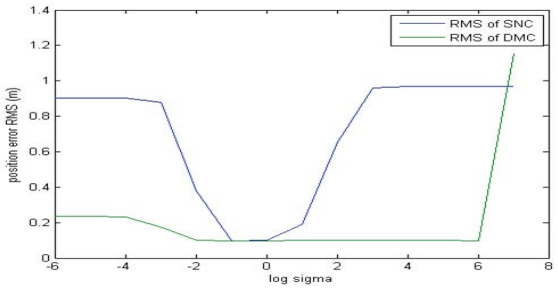


Fig.5. RMS value for position error as a function of $\sigma$

As observed from Fig.5, in comparison to SNC, which is observed to be significantly sensitive towards varying $\sigma$, DMC offers significant performance over a considerable broader $\sigma$ range.

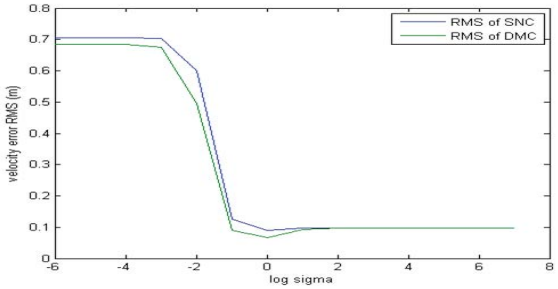


Fig.6. RMS value for velocity error as a function of $\sigma$

Furthermore, Fig.6 shows, over a broader $\sigma$ range, DMC offers comparatively refined approximation of

velocity than SNC. This proves DMC is comparatively more stable than SNC and thus, better choice for use in orbit determination.

## III. EXTENSION

### A. 2nd-order DMC Algorithm

From comparison of DMC with SNC, it is deduced that DMC offers considerable advantages. Although, choice of setting the acceleration, which is undetermined, to be 1st-order differential equation is quite arbitrary, a 2nd-order DMC algorithm is set up to assess DMC with differential equation of higher order. This implies, an assumption is made regarding characterization of undetermined acceleration to be 2nd-order differential equation:

$$\ddot{\eta}(t) = \alpha\dot{\eta}(t) + \beta\eta(t) + u(t) \tag{10}$$

Also, the vector of state deviation is

$$X = \begin{bmatrix} X \\ \dot{X} \\ \eta \\ \dot{\eta} \end{bmatrix} \tag{11}$$

Where, $X$ and $\dot{X}$ represents the position and velocity vector respectively. Optimization is carried out on constants $\alpha$ and $\beta$ to determine the best approximation. Once more, 2nd-order DMC algorithm is used to compute the results from the example mentioned earlier and compare to those of DMC. As per the example, the equations are

$$\dot{x}(t) = A(t) + x(t) + B(t)u(t); X = \begin{bmatrix} X \\ V \\ \eta \\ \dot{\eta} \end{bmatrix};$$

$$A = \begin{bmatrix} 0 & 1 & 0 & 0 \\ 0 & 0 & 1 & 0 \\ 0 & 0 & 0 & 1 \\ 0 & 0 & \beta & \alpha \end{bmatrix}; B = \begin{bmatrix} 0 \\ 0 \\ 0 \\ 1 \end{bmatrix};$$

$$E[u] = 0; E\left[uu^T\right] = \sigma^2 \tag{12}$$

Best approximation for position and velocity for 2nd-order DMC + Kalman filter system is presented in Fig.7. For accomplishing most optimized results, the considered values are: $\alpha$ is -0.66, $\beta$ is 0.10, and $\sigma$ is 0.95, RMS value for position error is $9.83*10^{-2}$ meter, and the RMS value for velocity error is $6.13*10^{-2}$ meter/second. It's been observed from the RMS results, even though 2nd-order DMC yields approximately similar position approximation with DMC, it does provide better velocity approximation.

However, defined 2nd-order DMC tend to deliver comparatively better unmodeled acceleration approximation. Fig.8 demonstrates the comparison between the results obtained. Acceleration computed by 2nd-order DMC, in comparison to DMC, is determined to be smoother on slopes and the RMS value for acceleration error, which is $1.806*10^{-1}$ meter/second$^2$, in comparison to DMC, is substantially smaller.

In Table II summarized RMS value of position error, velocity error, and acceleration error for different methods used is illustrated, which clearly demonstrates 2nd-order DMC yields comparatively more accurate approximation of velocity and acceleration, than SNC as well as DMC.

Additionally, stability assessment of 2nd-order DMC is also performed. For both DMC and 2nd-order DMC, comparative assessment of computed values for position error RMS along with velocity error RMS for $\log(\sigma) = [-6:1:7]$ is presented in Fig.9 and Fig.10.

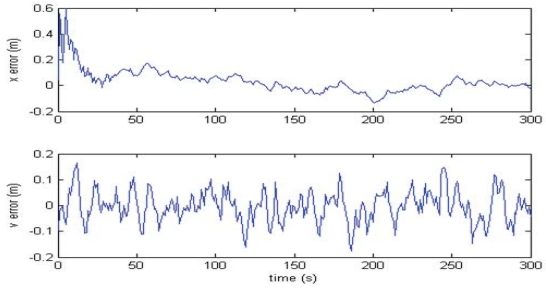


Fig.7. 2nd-order DMC + Kalman filter-based error estimation for position and velocity

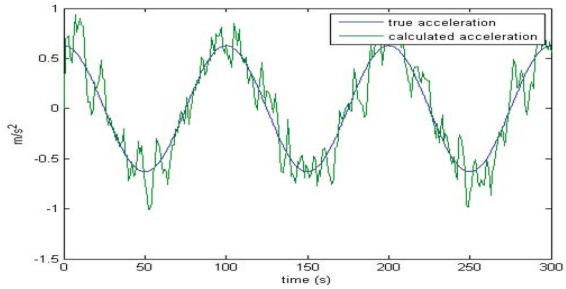


Fig.8. 2nd-order DMC + Kalman filter-based comparative analysis between unmodeled and calculated acceleration

TABLE II. SUMMARIZED RMS VALUE OF POSITION ERROR, VELOCITY ERROR, AND ACCELERATION ERROR FOR DIFFERENT METHODS

| Parameter | SNC | DMC | DMC of 2nd-Order |
|---|---|---|---|
| RMS value for position error (meter) | $9.83*10^{-2}$ | $9.83*10^{-2}$ | $9.83*10^{-2}$ |
| RMS value for velocity error (meter/second) | $7.57*10^{-2}$ | $6.78*10^{-2}$ | $6.13*10^{-2}$ |
| Acceleration error RMS (meter/second$^2$) | N/A | $2.424*10^{-1}$ | $1.806*10^{-2}$ |

For eliminating complexity in code, $\alpha$ and $\beta$ are set to optimal values, $\sigma$ is changed for computation while utilizing DMC of 2nd-order, while further optimizing $\beta$ for distinct $\sigma$ values for DMC. Thus, incase $\alpha$ and $\beta$ are further optimized for distinct $\sigma$ values for DMC of 2nd-order, the resulting outcome will be further satisfactory.

Although, it is quite observable now that, in comparison to DMC, DMC of 2nd-order is more stable. However, in case of substantially large $\sigma$ values, along with RMS value for position error approximately 1.10 meters, as well as substantially large RMS value for acceleration error, DMC fails; although for DMC of 2nd-order, RMS value for position error as well as for acceleration error, goes through minor changes when $\sigma$ changes over broader range.

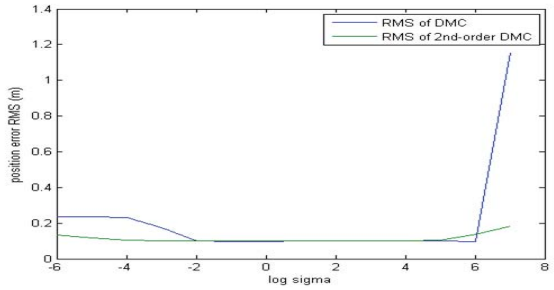


Fig.9. RMS value for position error as a function of $\sigma$

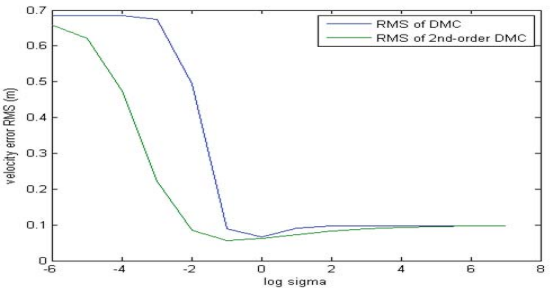


Fig.10. RMS value for velocity error as a function of $\sigma$

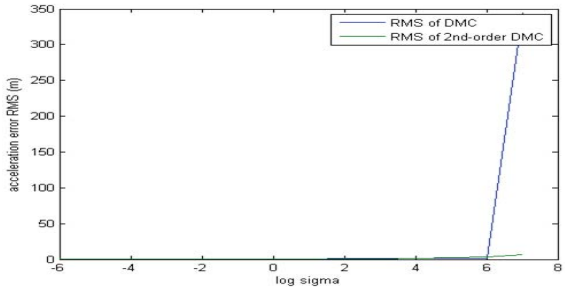


Fig.11. RMS value for acceleration error as a function of $\sigma$

### B. *Substandard Tracking based Simulation in presence of Unmodeled Acceleration*

For spaceflight missions like altimetric mission, measurement of POD nowadays is rather accurate and also it yields precise tracking information for determination of the orbit [17]. Although, for certain spaceflight missions, e.g. CubeSats, neither quality of the tracking data is up to the mark, nor dynamic models are freed from errors, thus making POD for such tasks very difficult. Hence, to work out such problem, 2nd-order DMC is applied.

Considering a situation where trajectory estimation for a CubeSat orbiting LEO needs to be carried out. For simplicity, to assure CubeSat orbit lies on x-y plane in Earth-Centered Inertial (ECI) coordinate system, CubeSat inclination is taken as 0°. For generating the monitoring data, 2-body equation of motion (EoM) is utilized in presence of perturbation of $J_2$ type inclusive of atmospheric drag effects. EoM inclusive of $J_2$ perturbation can be defined as:

$$\ddot{\vec{r}} = \nabla U \tag{13}$$

$$U = U_{point\,mass} + R$$

$$= \frac{\mu}{r}\left[1 - J_2\left(\frac{R_\oplus}{r}\right)^2\left(\frac{3}{2}\sin^2\varphi - \frac{1}{2}\right)\right] \tag{14}$$

Where latitude is defined in terms of $\varphi$ and hence in this case $\sin^2\varphi = 0$. Thus, the acceleration equations are described as

$$\ddot{r}_x = -\frac{\mu x}{r^3}\left(1 + \frac{3}{2}J_2\left(\frac{R_\oplus}{r}\right)^2\right) \tag{15}$$

$$\ddot{r}_y = -\frac{\mu y}{r^3}\left(1 + \frac{3}{2}J_2\left(\frac{R_\oplus}{r}\right)^2\right) \tag{16}$$

The acceleration equation in presence of atmospheric drag is given as [5]

$$\ddot{\vec{r}}_{drag} = -\frac{1}{2}\rho\left(\frac{C_D A}{m}\right)V_r^2\vec{u} \tag{17}$$

where $C_D$ = drag coefficient, $\rho$ = atmospheric density, $m$ = satellite mass, $A$ = cross-sectional area orthogonal to relative velocity vector = $\vec{V}_r$, $\vec{u}$ = unit vector along $\vec{V}_r$ direction, and $V_r$ = relative speed w.r.t the atmosphere. The parameter $\left(C_D A/m\right)$ is aka ballistic coefficient. For CubeSat, $C_D$ = 2.00, $m$ = 5.00 kg, and $A$ = 0.20 meter$^2$, and $\vec{V}_r = \left[V_x + \dot{\theta}_y, V_y - \dot{\theta}_x\right]$, where $\dot{\theta}$ = Earth's rotation angular velocity.

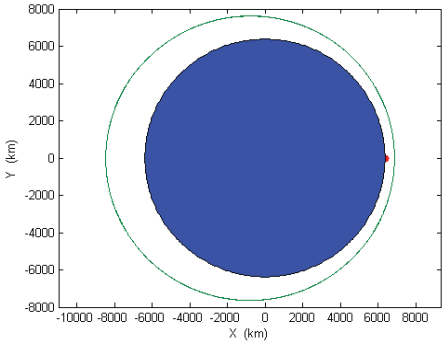


Fig.12. Orbit of CubeSat in x-y plane. Solid blue circle represents the Earth, green ring around it represents CubeSat orbit, and red colored point represent monitoring station location

For generating CubeSat's monitoring data, a dynamic model which consists of atmospheric drag along with $J_2$ perturbation is used [18]. Considering CubeSat initial orbit

to be at an altitude of 500 km i.e. LEO. For avoiding complexity CubeSat's initial position in the LEO is set as $x = \mathrm{R}_{Earth} + 500 = 6,878.14$ km, $y = 0.00$ km, and $z = 0.00$ km; initial velocity, $V_x = 0.00$ km/second, $V_y = 8.00$ km/second, $V_z = 0.00$ km/second. Furthermore, monitoring station is considered to be located at $x = \mathrm{R}_{Earth}$ km, $y = 0.00$ km, $z = 0.00$ km and range monitoring can only be performed once every 10 seconds. MATLAB's ode45 function is taken in account to integrate, compute range of the observation, and include white noise with zero mean value and $\sigma$ = 0.10 km. For CubeSat, $a$ = 7,679.60 km, $e$ = 0.1044, $i$ = 0°, and true anomaly = 0°, are the initial orbital elements. Fig.12 depicts orbit of CubeSat in x-y plane which follows ECI coordinate system. The monitoring data generated, inclusive of 4 passes are conveyed as:

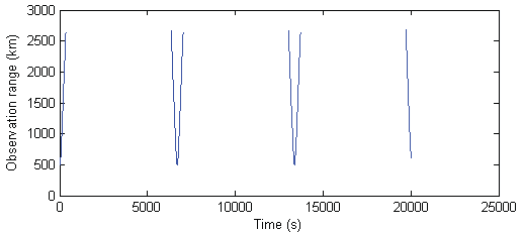


Fig.13. CubeSat's monitoring range data

Due to close range presence of monitoring station to the perigee point in the orbit of CubeSat, monitoring data are observed to be noisy and sparse, hence, allowing the performance examination of 2nd-order DMC + Kalman filter in presence of substandard tracking information. Unavailability of sufficient data are the reason why standard Kalman filter is chosen over EKF, which is known for efficiently performing in altimetric missions, but stays non-operational for initial observations. For simulating real-time scenario comprising of multiple errors within dynamic models, while executing algorithms for determining orbits, 2-body equation accompanied by $J_2$ perturbation as dynamic model is used exclusively.

Residuals (= estimation - observation) estimation plot on exclusive application of Kalman filter is presented in Fig.14.

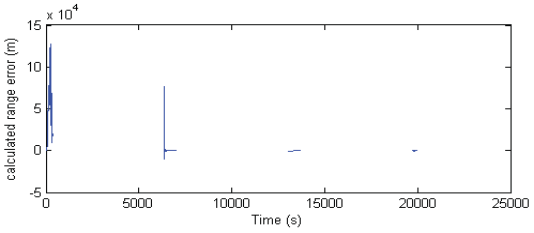


Fig.14. Kalman filter applied 4 passes-range residuals plot.

At this stage it is observed, for stability, CKF demands multiple passes information due to the reason that observation information is noisy and sparse. Consequently, during the 3rd pass, two algorithms are applied and results are compared. In fig.15, standard Kalman filter applied 3rd pass-range residuals are presented, which are deduced to be significantly large, having RMS value of 562.17 meters.

For 2nd-order DMC algorithm + Kalman filter, the desired equations are:

$$\frac{dx}{dt} = A(t).x(t) + B(t).u(t) \tag{18}$$

$$u = \begin{bmatrix} u_x \\ u_y \end{bmatrix} \tag{19}$$

$$\frac{d^2\eta_x}{dt^2} = a_x.\frac{d\eta_x}{dt} + \beta_x.\eta_x(t) + u_x(t) \tag{20}$$

$$\frac{d^2\eta_y}{dt^2} = a_y.\frac{d\eta_y}{dt} + \beta_y.\eta_y(t) + u_y(t) \tag{21}$$

And the standard deviation of $u_x$ is $\sigma_x$, and $u_y$ is $\sigma_y$. The state vectors used are presented in the following column as

$$X = \begin{bmatrix} X \\ Y \\ V_x \\ V_y \\ \eta_x \\ \eta_y \\ \dot{\eta}_x \\ \dot{\eta}_y \end{bmatrix}, A = \frac{\partial X}{\partial X}, B = \begin{bmatrix} 0 & 0 \\ 0 & 0 \\ 0 & 0 \\ 0 & 0 \\ 0 & 0 \\ 0 & 0 \\ 1 & 0 \\ 0 & 1 \end{bmatrix} \tag{22}$$

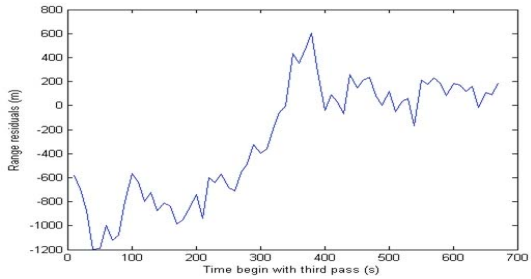


Fig.15. Kalman filter applied 3rd pass-range residuals

Once, after $t \approx 3.6$ hours, Kalman filter acquires relative stability, 2nd-order DMC algorithm is applied. For simulating it to real-time scenario arbitrary values are chosen for all the constants. 2nd-order DMC algorithm + Kalman filter applied range residuals are presented in Fig.16.

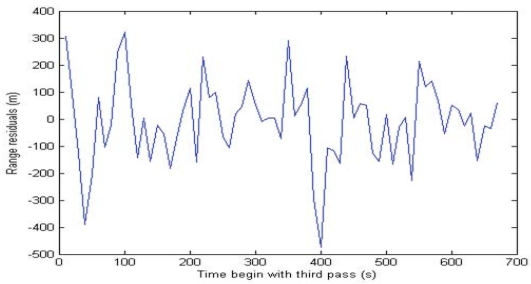


Fig.16. 2nd-order DMC + Kalman filter applied 3rd pass-range residuals

($\sigma_x$, $\sigma_y$) values are ($1*10^{-8}$, $1*10^{-8}$), ($\alpha_x$, $\alpha_y$) values are ($-1*10^{-2}$, $-1*10^{-2}$ ), and ($\beta_x$, $\beta_y$) values are ($1*10^{-2}$, $1*10^{-2}$). Range residuals RMS value comes out to be 146.6764 meters, which is significantly small in comparison to values obtained when only Kalman filter is applied. To make results more profound additional efforts are required for optimization of constants. Although optimization process can cause reduction in efficiency.

### C. Extension based Recommendations

For extension part, 2nd-order DMC algorithm is defined in order to make comparison to SNC and DMC. Results stated that 2nd-order DMC algorithm is more stable and tend to deliver comparably better precise estimation. Although, one drawback with such algorithm is its reliance on multiple parameters, which eventually increases the complexity for tuning process. In addition to this, in comparison to other algorithms, parameters for state vectors required by 2nd-order DMC are high, thus, eventually lowering the computational efficiency. All things considered, use of 2nd-order DMC is still recommended for dynamic model error compensation due to its better performance even with substandard tracking data.

## IV. Conclusion

In this research, discussion has been carried out on the methods that can be used for compensating errors present in dynamic models for POD. On analysis, results revealed both the algorithms, SNC and DMC, can not only substantially boost Kalman's filter performance, but yield more precise position estimation. However, on comparing results of two algorithms within themselves it is observed that DMC holds an upper hand over SMC in terms of more precise velocity estimation, precise acceleration estimation, and stability. As an extension, 2nd-order DMC algorithm is defined in order to make comparison to SNC and DMC. Results stated that 2nd-order DMC algorithm is more stable and tend to deliver comparably better precise estimation of position, velocity, and acceleration. In addition to this, 2nd-order DMC is highly recommended for dynamic model error compensation due to its better performance even with substandard tracking data and capability to deliver relatively precise position estimation. Hence, inclusion of 2nd-order DMC algorithm within Kalman filter for error compensation in dynamic models in POD problems is strongly recommended.

## References


[1] S. Bruinsma, S. Loyer, J. M. Lemoine, F. Perosanz, and D. Tamagnan, "The impact of accelerometry on CHAMP orbit determination," Journal of Geodesy, Vol. 77, Issue 1-2, pp. 86-93, 2003.

[2] S. B. Luthcke, N. P. Zelensky, D. D. Rowlands, F. G. Lemoine, and T. A. Williams, "The 1-centimeter orbit: Jason-1 precision orbit determination using GPS, SLR, DORIS and altimeter data," Marine Geodesy, Vol. 26, Issue 3-4, pp. 399– 421, 2003.

[3] D. Gaur, M. S. Prasad, "One-second GPS orbits: A comparison between numerical integration and interpolation," 6th International Conference on Signal Processing and Integrated Networks, pp. 973-977, 2019.

[4] B. S. Schutz, L. Bae, R. Magruder, R. Rickletfs, E. Rim, Silverberg, C. Webb, and S. Yoon, "Precision orbit and attitude determination for ICESat," Advances in Astronautical Sciences, Vol. 115, pp. 416-427, 2003.

[5] B. D. Tapley, B. E. Schutz, J. C. Ries, and C. K. Shum, "Precision orbit determination for TOPEX," Adv. Space Res., Vol. 10, Issue 3-4, pp. 239-247, 1990.

[6] B. D. Tapley, J. C. Ries, G. W. Davis,R. J. Eanes, B. E. Schutz, C. K. Shum, and M. M. Watkins, "Precision orbit determination for TOPEX/POSEIDON," J. Geophys. Res., Vol. 99, Issue C12, pp. 24,383-24,404, 1994.

[7] D. R. Cruickshank, "Genetic Model Compensation: Theory and Applications," Ph. D. Dissertation, The University of Colorado at Boulder, 1998.

[8] B. D. Tapley, B. E. Schutz, and G. H. Born, "Statistical Orbit Determination," Elsevier Academic Press, New York, 2004.

[9] F. H. Schlee, C.J. Standish, and N.F. Toda, "Divergence in the Kalman filter," AIAA Journal, Vol. 5, Issue 6, pp. 1114–1120, 1967.

[10] D. Gaur, M. S. Prasad, "Optimal gravity assisted orbit insertion for Europa orbiter mission," International Journal of Application or Innovation in Engineering & Management, Vol. 7, No. 8, pp. 055-062, 2018.

[11] D. S. Ingram, B. D. Tapley, "Lunar orbit determination in the presence of unmodeled accelerations," Celestial Mechanics, Vol. 9, Issue 4, pp. 191-211, 1974.

[12] B. D. Tapley, and D. S. Ingram, "Orbit determination in the presence of unmodeled accelerations," IEEE Transactions on Automatic Control, Vol. 18, Issue 4, pp. 369-373, 1973.

[13] C. L. Lawson, and R. J. Hanson, "Solving least squares problem," Prentice-Hall, EnglewoodCliffs, NJ, 1974.

[14] D. Gaur, M. H. Lowenberg, M. S. Prasad, "Assessing nonlinear robustness of control law designs," 6th International Conference on Signal Processing and Integrated Networks, pp. 932-938, 2019.

[15] D. Gaur, M. S. Prasad, "Optimal interplanetary trajectories for solar sail," International Journal of Application or Innovation in Engineering & Management, Vol. 7, No. 8, pp. 093-100, 2018.

[16] D. Gaur, M. S. Prasad, "Optimal control based time optimal low thrust orbit raising," International Journal of Application or Innovation in Engineering & Management, Vol. 7, No. 8, pp. 077-082, 2018.

[17] D. Gaur, M. S. Prasad, "Revisiting apollo laser altimetry with modern lunar gravity models," International Journal of Application or Innovation in Engineering & Management, Vol. 7, No. 8, pp. 069-076, 2018.

[18] F. A. Marcos, C. R. Baker, J. N. Bass, T. L. Killeen, and R. G. Roble RG, "Satellite drag models: current status and prospects," Advances in the Astronautical Sciences, Vol. 85, No. pt 2, pp. 1253-1273, 1993.